The Characteristics of Soot Formed in Premixed Flames by Different Fuels

Carmela Russo[a] (lina.russo@virgilio.it), Fernando Stanzione[b] (f.stanzione@irc.cnr.it), Rosalba Barbella[b] (barbella@irc.cnr.it), Antonio Tregrossi[b] (treg@irc.cnr.it), Anna Ciajolo[b] (ciajolo@irc.cnr.it)

[a] Dipartimento di Ingegneria Chimica, Università Federico II, P.le V. Tecchio, 80 - 80125, Napoli, ITALY
[b] Istituto di Ricerche sulla Combustione - C.N.R, P.le V. Tecchio, 80 - 80125, Napoli, ITALY

The internal structure of soot sampled from fuel-rich methane and benzene premixed flames burning in different temperature conditions was investigated. UV-visible spectroscopy was used for its sensitivity to the carbon network in terms of sp^2 and sp^3 sites and of extension of sp^2 aromatic moieties. The UV-visible absorption maximum and the optical band gap have shown to be affected by the fuel characteristics rather than by flame temperature. The important role of fuel aromaticity on soot internal structure from particle inception throughout the soot formation region was demonstrated.

Introduction

Carbonaceous aerosols, largely produced from the combustion of fossil fuels and widely distributed in the atmosphere, affect the solar input to the earth–atmosphere system by scattering and absorbing radiation and by providing sites for the condensation of clouds. Thus, the optical properties as well as the number size distribution of combustion-formed carbonaceous particles determine their role in climate change governing the radiative forcing and their study is important to foresee and model how aerosols affect the environment. Previous works have yielded a wide range of values for the absorptive properties of light-absorbing carbon (Bond and Bergstrom, 2006), that is generally termed soot in combustion science and by the Intergovernmental Panel on Climate Change (IPCC, 1996). Absorptive properties of carbon materials as soot are known to mainly depend on the molecular form. In particular the size of sp^2-bonded clusters, constituting the aromatic units of soot, affects the absorption spectra. The size of sp^2-bonded clusters, as well as the number of sp^2 and sp^3 sites contained in soot, are induced by diverse combustion conditions and different fuels (Tregrossi et al., 2007; Apicella et al., 2004). It derives that the effect of combustion parameters on the absorptive properties of soot at the exhaust has to be studied to provide the input parameters for aerosol modelling also in view of further modifications of soot in the atmosphere. UV-visible spectroscopy can be used as probe of the sp^2 clusters mainly ruling the electronic properties of carbon materials (Jager et al., 1999). In this work the position of the UV-visible absorption maximum and the spectral shape of soot have been measured to

follow the size variation of the aromatic clusters in premixed sooting flames of methane and benzene in different flame temperature conditions from soot inception up to the final stage of soot formation and emission.

1. Experimental

Measurements have been carried out on laminar premixed flames at atmospheric pressure produced on a commercial McKenna burner. The flame conditions are reported in Tab.1. The particulates have been also caught on quartz plates inserted in the soot formation region at different heights above the burner (HAB) for the minimum time (600ms) required both to collect a sufficient material for the spectroscopic analysis and to limit the thermal degradation of the deposited sample. The particulate deposited on the quartz plate has been washed with dichloromethane (DCM) in order to measure the UV-visible spectrum of the residual carbon soot particles devoid of the condensed species adsorbed on it. UV–visible absorption of soot deposited on quartz plates was measured in the 190-800nm wavelength range on an HP8452A spectrophotometer.

Table 1 Flame operating conditions

Parameters	Flame#1	Flame#2	Flame#3	Flame#4
C/O ratio	0.6	0.6	0.8	0.8
Fuel	Methane (54.5%)	Methane (54.5%)	Benzene (5.7%)	Benzene (5.7%)
Diluent	-	-	N_2 (72.6%)	N_2 (72.6%)
Cold gas velocity, cm/s	4	5	3	4
T max, K	1650 at 2.2mm	1770 at 2.2mm	1720 at 3.7mm	1830 at 3.3mm

2. Results

The relationship between specific features of UV-visible spectra with carbon bonding characteristics can be exploited for obtaining information on soot internal structure. The UV-visible absorption is caused by electronic transitions between the bonding and antibonding orbitals. The σ-σ* transitions, typical of sp^3 hybridization, are expected to produce a band in the far UV toward 100nm, whereas the π-π* transitions, due to sp^2 hybridization, provide an absorption maximum located between 180 and 280nm (Llamsa-Jansa et al., 2007). The position of the π-π* transition is extremely sensitive to small variations in the internal electronic structure of the carbon particles (Robertson&O'Reilly, 1987). In particular it has been assessed that the UV band position of carbon black, that somehow presents many similarities with soot particles, has shown to be strictly related to the internal structure of the particles and especially to the sp^2/sp^3 character. (Jager et al. 1999; Llamas-Jansa et al. 2007; Mennella et al., 1995). It has been shown that the peak position shifts toward the visible as the sp^2 character increases and as the growth of the graphene sp^2 layers occurs. The absorption spectra of soot caught on quartz plates inserted along the axis of fuel-rich premixed flames of methane and benzene, reported in Fig. 1 and Fig. 2, respectively, are focused in the UV region (200-400nm wavelength region) to follow in detail the UV band position. In methane flames soot inception occurs in the post-oxidation flame region at

6mm HAB (Fig. 1), whereas in benzene flames earlier soot inception occurs at about 3-4mm HAB corresponding to the end of the main oxidation region (Fig. 2).
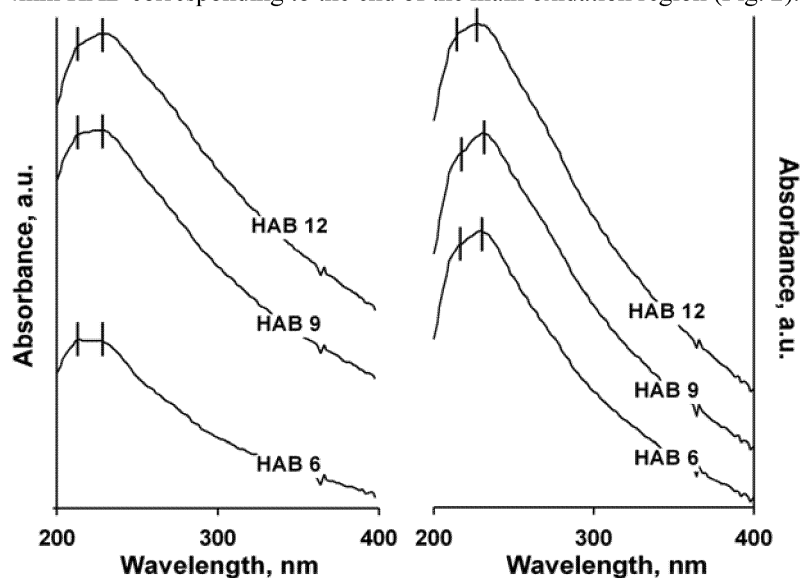

Figure 1 UV-visible spectra of the particulates deposited at different heights above the burner in the methane flame#1 (left part) and in the methane flame #2 (right part)

The steep rise of UV-visible absorbance, due to the increase of soot concentration, occurs to 12mm HAB in both methane and benzene flames marking the end of soot formation region. The spectra present the main band focused in the UV, followed by the steady decrease of absorbance toward the visible typical of carbon materials. Some spectral differences, described in the following, can be noted as soot ages and as function of the fuel. In the methane flame#1 (left part of Fig.1) the UV absorption band exhibits two maxima of comparable intensity at 214nm and 230nm. At increasing flame heights, the UV band focus on 230nm maximum (Tregrossi and Ciajolo, 2010). In the higher temperature conditions of the methane flame#2 (right part of Fig.1), UV-visible spectra present a constant maximum of absorption at about 230nm with a lower contribution of the 214nm maximum. In the benzene flame#3 (left part of Fig. 2) the UV band is located at higher wavelengths (230-246nm) and the 246nm absorption maximum becomes predominant along the flame. At the higher temperature of the benzene flame # 4 (right part of Fig. 2) the UV band appears sharper with the maximum absorption located upward at 230nm and slightly shifting toward the visible (240nm) along the flame. Overall, it can be assessed that the UV absorption band is generally located at lower wavelengths in methane flames with respect to benzene flames. Remembering that a UV band located at lower wavelengths corresponds to lower sp^2 aromatic character and size, these findings demonstrate that the internal structure of methane soot presents a lower graphitization degree in respect to benzene soot presenting a higher graphitization degree already at soot inception. It is noteworthy that the temperature increase does not affect the UV position in methane flames whereas it causes the backward shift of UV band in benzene flames. Indeed, in methane flames the aromatic precursors and soot are formed in the post-oxidation region where hydrogen

and aliphatic hydrocarbons are largely present and temperature is steadily decreasing (Alfè et al. 2010).
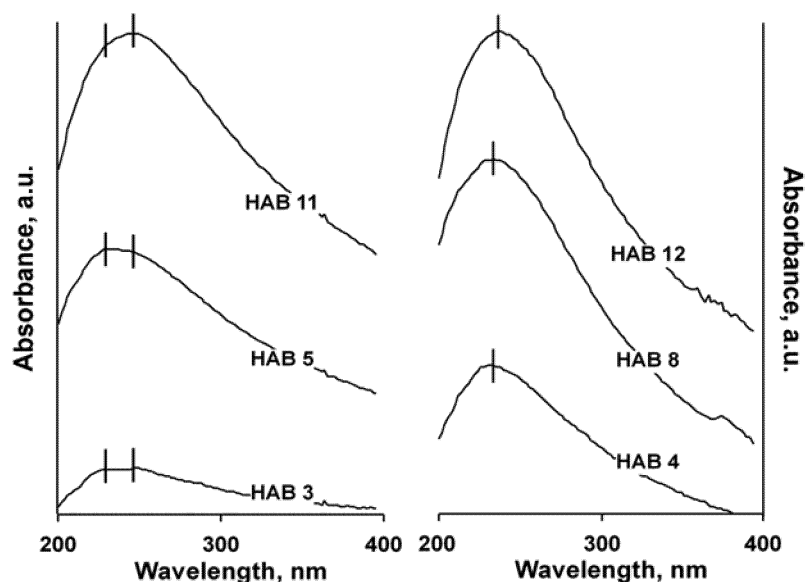

Figure 2 UV-visible spectra of the particulates deposited at different heights above the burner (HAB) in the benzene flame#3 (left part) and in the benzene flame#4 (right part)

This causes a slower growth of the size of sp^2 layers, not significantly affected by the temperature, with a consequent localization of π and π^* electronic band, often interrupted by aliphatics and hydrogen deriving from methane pyrolysis. Similarly, it is the flame structure determining the internal structure and graphitization degree of benzene soot. Indeed, soot formation in benzene flames occurs at high temperature in the main oxidation flame region, rich of radicals and aromatic species coming from fuel oxidation/pyrolysis (Tregrossi et al. 1999). In these conditions highly-graphitized soot is rapidly formed through condensation radical reactions between aromatics favoured by the high hydrogen radical concentration The higher graphitic character of benzene soot is confirmed by the lower hydrogen content of benzene soot in respect to soot produced by aliphatic fuels (Alfè et al., 2009). However, the unexpected backward shift of the UV band of benzene soot at higher temperatures can be due to the lower residence time (higher cold gas velocity), associated to the higher temperature conditions that do not favour the growth of sp^2 layers. However, it has to be underlined that other factors, as the bending of sp^2 layers or aggregation, can cause the shift toward UV of the maximum absorption (Jager,1999). Further work is thus necessary to verify the source of the temperature effect on benzene soot structure. From the examination of spectra reported in Figs.1-2 it can be also noted that the absorption is more extended toward the visible as soot ages along the flame and in particular in the benzene flames.

The energy band gap, adopted in the UV absorption model of Robertson (1991) and Robertson and O'Reilly (1987) for the analysis of amorphous carbons, gives the evaluation of these spectral changes, being a spectral signature of the size distribution of the aromatic islands. The energy band gap parameters have been evaluated on the whole 200-800 nm wavelength range spectra measured in the methane and benzene flames,

following the Tauc relation (1) (Tauc et al., 1966) linking the absorbance with energy band gap (E_g):

$$(\alpha E)^{1/2} = B(E-E_g) \tag{1}$$

where E is the energy of the incident photon and B is a constant. Using the Tauc representation it was not possible to identify an unique energy band gap in the measured spectra because the slope of the curve significantly changes in the 200-800 nm region. This finding gives evidence of the presence of different classes of absorbers in soot particles responsible for the energy band gap named E_{g1}, E_{g2} and E_{g3} (Minutolo et al., 1996; Tregrossi and Ciajolo, 2010). The lowest E_{g1} (0.1-1) of class 1, reported in the left part of Fig. 3, is typical of large graphitized structures (Eg of graphite is 0) aborbing up to the highest limit of absorption spectra (800 nm). The intermediate E_{g2} value (about 2) of class 2, reported in the middle part of Fig. 3, corresponds to intermediate aromatic systems (>10 rings for compact pericondensed aromatics), absorbing up to about 500nm, whereas the lowest value of E_{g3} (about 4) of class 3, reported in the right part of Fig. 3, is due to low aromatic size components as 2-7 ring polycyclic aromatic hydrocarbons, absorbing up to about 250nm. It is noteworthy that E_{g2} and E_{g3} values are not affected by neither fuel or temperature. Conversely, the E_{g1} gap shows to be strongly affected by the fuel being the E_{g1} value of benzene soot much lower than that of methane soot. The low Eg values correspond to a large size of aromatic absorbers, thus the lowest E_{g1} values of benzene soot indicates that the graphitization of benzene soot is generally much higher already at soot inception. Moreover, it is noteworthy that the flame temperature does not significantly affect the E_{g1} values confirming that fuel identity rather than temperature affects soot internal structure.
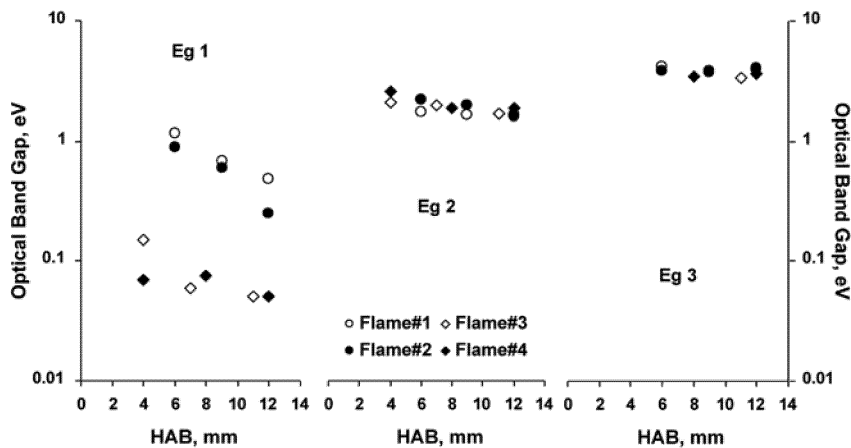

Figure 3 Optical band gaps of the three classes of absorbers evaluated on soot along the axis of the different flames: Eg1 in the left part, Eg2 in the middle part and Eg3 in the right part

3. Conclusions

The analysis of the optical feature of soot sampled from methane and benzene premixed flames, burning in fuel rich conditions at similar temperatures, has been carried out. The

spectroscopic properties, in particular the uv-resonance band wavelength and the optical gap, have shown to be affected by the fuel characteristics and by the reciprocal position of the pyrolysis and oxidation zone. The results seems to confirm the fundamental role of fuel nature, specifically fuel aromaticity, on the particle inception and mass growth processes during the early stages of soot formation, that has to be attributed to a different pathways of soot inception also due to the overlapping of the pyrolysis and oxidation regions in benzene flames.

References

Alfè, M., Apicella, B., Barbella, R., Rouzaud, J. N., Tregrossi, A., Ciajolo, A., 2009, Structure–property relationship in nanostructures of young and mature soot in premixed flames Proc. Combust. Inst. 32, 697-704.

Alfè, M., Apicella, B., Rouzaud, J. N., Tregrossi, A., Ciajolo, A., 2010, The effect of temperature on soot properties in premixed methane flames, Combust. And Flame (2010), doi:10.1016/j.combustflame.2010.02.007, in press.

Apicella, B., Alfè, M., Barbella, R., Tregrossi, A., and Ciajolo, A., 2004, Aromatic structure of carbonaceous materials and soot inferred by spectroscopic analysis, Carbon 42, 1583-1589.

Bond, T. C., Bergstrom, R. W., 2006, Light absorption by carbonaceous particles: An investigative review, 2006, Aerosol Science and Technology 40, 27-67.

Jager, C., Henning, T., Schlö̈gl, R., and Spillecke, O., 1999, Spectral properties of carbon black. Journal of Non-Crystalline Solids 258, 161-179.

Llamas-Jansa, I., Jager, C., Mutschke, H., Henning, Th., 2007, Far-ultraviolet to near-infrared optical properties of carbon nanoparticles produced by pulsed-laser pyrolysis of hydrocarbons and their relation with structural variations, Carbon 45, 1542-1557.

Mennella, V., Colangeli, L., Bussoletti, E., Monaco, G., Palumbo, P., and Rotundi, A., 1995, On the electronic structure of small carbon grains of astrophysical interest. APJS 100, 149-157.

Minutolo, P., Gambi, G., and D'Alessio, A., 1996, The optical band gap model in the interpretation of the uv-visible absorption spectra of rich premixed flames. Proc.Combust. Instit. 26, 951-956.

Robertson, J., 1991, Hard amorphous (diamond-like) carbons. Prog. Solid St. Chem. 21, 199-333.

Robertson, J., and O'Reilly, E.P., 1987, Electronic and atomic structure of amorphous carbon. Phys. Rev B 35, 2946-2957.

Schnaiter, M., Mutschke, H., Dorschner, J., Henning, T., and Salama, F., 1998, Matrix-isolated nano-sized carbon grains as an analog for the 217.5 nanometer feature carrier, APJ 498, 486-496.

Tauc, J., Grigorovici, R., and Vancj, A., 1966, Optical properties and electronic structure of amorphous germanium. Phys. Stat. Sol. 15, 627-637.

Tregrossi, A., Ciajolo, A., Barbella, R., 1999, The Combustion of Benzene in Rich Premixed Flames at Atmospheric Pressure, Combust. and Flame 117, 553-561

Tregrossi, A., Barbella, R., Ciajolo, A., and Alfe`, M., 2007, Spectral properties of soot in the uv-visible range. Combust. Sci. and Tech. 179, 371-385.

Tregrossi, A, and Ciajolo, A., 2010, Spectral Signatures of Carbon Particulate Evolution in Methane Flames, Combust. Sci. and Tech. DOI: 10.1080/00102200903466517